Supporting Information

Ingham et al. 10.1073/pnas.1102097108

SI Materials and Methods

Strains and Culture. *Paenibacillus vortex* was grown as previously described (1). Spores of *P. vortex* were obtained by liquid culture in Difco sporulation medium, heat-killing vegetative cells (15 min at 80 °C), and purification, as previously described (2). *P. polymyxa* E681 (3) was grown under identical conditions as *P. vortex*. *Proteus mirabilis* JBZ2G (4) and an azole-sensitive (ITZ^-) strain of *Aspergillus fumigatus* 114 (5, 6) were obtained and routinely cultured as cited. *Penicillium citrinum* S12 (7), *P. expansum* BFE189 (6), *P. camemberti* LCP66.584 (8), and *Colletotrichum* gloeosporoides f. sp. *aeschynomene* 3.1.3 (9) were obtained as cited and cultured on Soya Mannitol agar (10) at 28 °C for 5 d to obtain conidia.

Conidial Germination and Outgrowth During Transport. The ability of conidia (asexual fungal spores) of *A. fumigatus* to germinate on reduced strength Mueller–Hinton agar (RMHA) without the presence of bacteria compared with those conidia transported by *P. vortex* on RMHA was determined by recovery with a toothpick and mounting on a microscope slide followed by observation by transmission light microscopy. Conidia were scored as ungerminated or germinated (larger diameter because of water uptake but no outgrowth) or with outgrowth as previously described (6).

Recovery and Selective Plating. To assess the colonization of different regions of agar plates by bacteria or *A. fumigatus*, regions of interest were excised with a razor blade or sterile pipette and homogenized, and selective viable counts were made. Viable counts of *P. vortex* or *P. mirabilis* were determined by plating on RMHA containing 0.5 mM *p*-nitrophenyl glycerol (PNPG; to inhibit swarming) and 5 μg mL^{-1} voriconazole where required to inhibit fungal growth. Counts of *A. fumigatus* were done by plating on Sabouraud agar. Incubations in all cases were at 37 °C for 18 h.

Staining Cells and Spores. A preparation of 2-*p*-iodophenyl-3-*p*-nitrophenyl-5-phenyltetrazolium chloride (INT) dissolved in water (1 mg mL^{-1}) and filter-sterilized was used to stain *P. vortex* on plates by spraying evenly using an atomizer. Plates were incubated 10 min at 37 °C before photographing or imaging. Staining vegetative cells with the fluorogenic dyes Syto 9 or hexidium iodide (Invitrogen) after recovery of mixtures of spores and cells by toothpick was as previously described (11). Selectively staining *P. vortex* in the presence of fungal hyphae used hexidium iodide delivered in aliquots of <1 μL by pipette or fine sable brush (Windsor and Newton) targeted by a dissection microscope.

Imaging. An Olympus BX-41 camera equipped with ×4, ×10, and ×50 Fluorotar lenses was used to image agar plates using transmission or digital interference contrast as appropriate. For quantification of fungal microcolonies, an acetate transparency printed with concentric rings, and sampling locations were placed under the agar plate to direct counting at random locations at desired distances from the central inoculation point. Preparation of *P. vortex* and mycelia from air gaps by fluorescence microscopy was staining with hexidium iodide in situ (described in the previous section) and then excising the region of interest from the agar plate, taking a small piece of the agar from either side of the gap with a fine scalpel. Such recovered samples were mounted inverted on a microscope slide for imaging. Visualization of mycelia across air gaps used a Leica DSZ dissecting microscope with illumination from above and a blue background under the agar plate to increase contrast for photography. The density of fungal microcolonies was assessed using low-magnification transmission light microscopy counting 20 3 × 4-mm fields of view per data point. Image capture was with a Kappa CCD camera. Image analysis and the assembly of stills into movies was made using ImageJ (version 1.41) (Movies S1, S2, and S3). Preparation of cells swarming on agar for scanning EM was by glutaraldehyde fixation and then treatment with osmium tetroxide and acetone dehydration, as previously described (1). Imaging after critical point drying and tungsten sputtering (2 nm) was done using a FEI Magellan scanning electron microscope.

Tracking and Modeling Bacterial and Conidial Motion. Image analysis and model creation was done using Matlab version 7.9. To capture the movement of a local group of bacteria and/or conidia within bacterial masses, pairwise comparisons were made between consecutive frames or frames separated by up to four other frames (depending on the speed at which the objects changed between frames). A small window (20 × 20 pixels) was moved over the first frame. A larger window (from 26 × 26 to 30 × 30 pixels) was moved over the second frame with an identical center point to the smaller window. The two windows from the two related frames were analyzed by fast normalized cross-correlation analysis (12). This algorithm gave a matrix of correlations corresponding to the similarity between all possible matches of the small window to the larger one. The highest correlation was used to determine the shift of the small window in the first frame relative to the bigger window in the second frame. This procedure was repeated for all windows in the same frame, with 50% overlap between windows, and all frames in the batch. By obtaining the velocity field of the bacteria, the direction of small groups of bacteria at any place in any given frame of the movie was assessed. Analyzing time development of the velocity maps enabled the study of new features. By using virtual beads, which follow the direction and speed of the bacterial mass, one can test the coupling between the mass and the conidia. The beads were placed within the velocity map near different conidia to check similarity between the trajectories. After the initial position, the virtual beads were allowed to move following the local direction of the velocity field at each frame. The trajectory and velocity of each virtual bead were compared with the trajectory and velocity of the nearest conidia (Fig. 3).

Treatment of *A. fumigatus* Conidia. The detergents SDS, Triton X-100, and Tween-20 at concentrations from 0.005% to 0.1% (wt/vol) were incubated with 10^9 conidia for 1 h at room temperature in 1 mL RMH broth (RMHB). Protease treatments with proteinase K or Pronase-E (all reagents from Sigma) were performed on the same number of conidia at 37 °C in PBS for 1 h with from 1,000 to 10,000 units/mL protease. After treatment, conidia were washed three times with RMHB by centrifugation before using in transport assays.

Purification of Flagella from Swarming Bacteria. Flagella were purified from *P. vortex* or *P. mirabilis* cells (10^{12}) swarming on RMHA plates. Flagella were sheared to remove them from the cells. Preparations were then centrifuged to remove the cells but leave the flagella in suspension followed by ultracentrifugation to concentrate the flagella as previously described (13). Flagella preparations (>95% pure as judged by SDS/PAGE) were quantified by Bradford assay and stored in sterile PBS at 4 °C.

Transport of Conidia into Locations Where Bacterial Growth Is Inhibited by Antibiotics. Niches of bacterial growth inhibition on RMHA plates were created by NeoSensi Tabs containing antibiotics [neomycin (NEO), vancomycin (VAN), linezolid, and trimethoprim]. All four antibiotics created zones of clearing (7–14 mm) when *P. vortex* was tested under nonswarming conditions on RMHA containing 0.5 mm PNPG. When *P. vortex* was inoculated outside the region of inhibition and permitted to swarm, then zones of growth inhibition were observed after 18 h. However, for all antibiotics tested, penetration of the zone of inhibition was possible by swarming bacterial aggregates up to 0.5 mm in diameter (Fig. S6). Such pioneering groups were able to traverse several centimeters of antibiotic impregnated agar to reach new areas favorable for growth. Tracking of these moving colonies suggested that these aggregates were not increasing in size while in the zone of inhibition (i.e., growth seemed limited). The refractory nature of the swarms to antibiotics was temporary. Isolation of cells from the swarms that penetrated the zone of inhibition followed by liquid culture without antibiotics and retesting indicated that antibiotic-resistant mutants were not being generated.

When inoculated in the center of the plate with conidia of *A. fumigatus*, pioneering groups of *P. vortex* were able to transport conidia into the regions of antibiotic action. In this situation, fungal outgrowth from the *P. vortex* colonies was rapid, and *A. fumigatus* rapidly came to dominate the niche (Fig. S7 *B* and *C*). Furthermore, 70 h after inoculation, conidiophore development was observed only within the zone in which the antibiotics limited *P. vortex* growth (Fig. S7*D*). Limiting growth of the bacterium with an antibiotic permitted *A. fumigatus* to develop to the point where conidiophores could be generated.

Transporter Specificity—Comparison with Other Swarming Bacteria. *P. polymyxa* swarmed at an average rate of 3.5 mm h^{-1} on RMHA, initiating swarming in 1–2 h. However, when co-inoculated with conidia of *P. citrinum*, swarming was initiated earlier (within 30 min) and was more rapid in the first 2 h (up to 7.1 mm h^{-1}). Transport was not observed for any conidia (including *P. citrinum* and *A. fumigatus*) using Difco or Eiken agars (0.7–2% wt/vol) using direct microscopy or microcolony growth as criteria. *P. mirabilis* JBZ2G swarmed up to 9.1 mm h^{-1} on RMHA. No significant dispersal of any of these fungal species was seen using colony development (36 h) or microcolony growth (16 h) as criteria when tested on RMHA plates using agars from Difco or Eiken [from 0.5% to 2% (wt/vol) agar in both cases]. Furthermore, transport of conidia of *A. fumigatus*, *P. camemberti*, *P. citrinum*, and *C.* gloeosporoides f. sp. *aeschynomene* by *P. mirabilis* was not observed by microscopy. Failure to transport conidia did not seem to be directly related to the consolidation of swarmer cells into vegetative cells. Conidia were not deposited in the first region where swarming cells differentiated into nonswarming vegetative cells. Rather, it appeared that swarming cells were simply unable to capture and transport conidia.

Effect of Transport on Germination and Outgrowth. To test the effect of the bacteria on postgermination outgrowth, the diameters of *A. fumigatus* microcolonies growing within an area of *P. vortex* growth on RMHA after 16 h were compared with the diameters of microcolonies produced after germination and outgrowth for 16 h on RMHA in the absence of bacteria. The average diameter (±SD) of *A. fumigatus* microcolonies was 167 ± 65 μm (n = 66) in the absence of bacteria and 53 ± 25 μm (n = 71) in the presence of *P. vortex*, suggesting that *P. vortex* inhibited the outgrowth of germinated microcolonies. However, development of aerial mycelia was still possible, and *A. fumigatus* was able to initiate growth within masses of *P. vortex*, grow out into regions not colonized by the bacteria (Fig. S7 *B* and *C*), and cross air gaps (Fig. 5).

1. Ingham CJ, Ben Jacob E (2008) Swarming and complex pattern formation in *Paenibacillus vortex* studied by imaging and tracking cells. *BMC Microbiol* 8:36.
2. Nicholson WL, Setlow P (1990) *Molecular Biological Methods for Bacillus*, eds, Harwood CR, Cutting S (Wiley, New York), pp 391–450.
3. Park S-Y, et al. (2008) Citrinin, a mycotoxin from *Penicillium citrinum*, plays a role in inducing motility of *Paenibacillus polymyxa*. *FEMS Microbiol Ecol* 65:229–237.
4. Budding AE, Ingham CJ, Bitter W, Vandenbroucke-Grauls CM, Schneeberger PM (2009) The Dienes phenomenon: Competition and territoriality in Swarming *Proteus mirabilis*. *J Bacteriol* 191:3892–3900.
5. Snelders E, et al. (2009) Possible environmental origin of resistance of *Aspergillus fumigatus* to medical triazoles. *Appl Environ Microbiol* 75:4053–4057.
6. Taubitz A, Bauer B, Heesemann J, Ebel F (2007) Role of respiration in the germination process of the pathogenic mold *Aspergillus fumigatus*. *Curr Microbiol* 54:354–360.
7. Schmidt-Heydt M, Geisen R (2007) A microarray for monitoring the production of mycotoxins in food. *Int J Food Microbiol* 117:131–140.
8. Giraud F, et al. (2010) Microsatellite loci to recognize species for the cheese starter and contaminating strains associated with cheese manufacturing. *Int J Food Microbiol* 137:204–213.
9. Robinson M, Riov J, Sharon A (1998) Indole-3-acetic acid biosynthesis in colletotrichum gloeosporioides f. sp. aeschynomene. *Appl Environ Microbiol* 64:5030–5032.
10. Arias ME, et al. (2003) Kraft pulp biobleaching and mediated oxidation of a nonphenolic substrate by laccase from *Streptomyces cyaneus* CECT 3335. *Appl Environ Microbiol* 69:1953–1958.
11. Ingham CJ, van den Ende M, Pijnenburg D, Wever PC, Schneeberger PM (2005) Growth and multiplexed analysis of microorganisms on a subdivided, highly porous, inorganic chip manufactured from anopore. *Appl Environ Microbiol* 71:8978–8981.
12. Lewis JP (1995) Vision interface 95. *Proceedings of the Canadian Image Processing and Pattern Recognition Society Meeting,* pp 120–123.
13. DePamphilis ML, Adler J (1971) Purification of intact flagella from *Escherichia coli* and *Bacillus subtilis*. *J Bacteriol* 105:376–383.

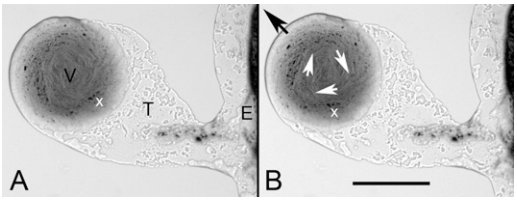

Fig. S1. Stills taken from Movie S2 showing mass spore transport by *P. vortex* by a rotating colony 2 h after inoculation. (*A*) E, exit point from the edge of inoculation; T, trail of cells and lubricant material; V, rotating colony. (*B*) Still of 20 s later. White arrows show clockwise rotation of colony, and black arrow shows overall direction of progress. (Scale bar: 0.4 mm.) Colony is rotating one time every 3 min, and conidial masses (e.g., the three dark objects marked X) are rotating at ~3 μm s^{-1}.

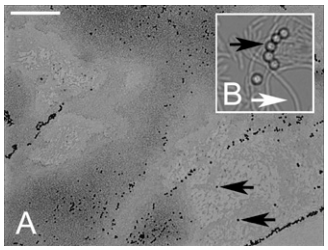

Fig. S2. (*A*) Swarming mass of *P. vortex* transporting hundreds of ungerminated conidia (individual conidia visible; e.g., as indicated by arrows). (*B*) High-magnification view of transported contidia (black arrow) with individual bacteria visible (e.g., white arrow). (Scale bar: *A*, 100 μm; *B*, 25 μm.)

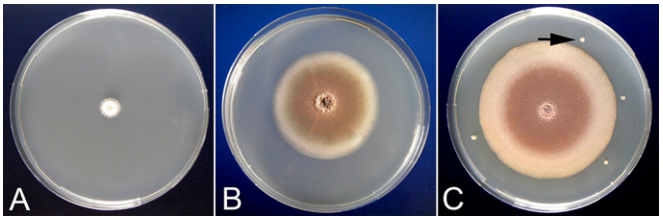

Fig. S3. Examples of growth of *A. fumigatus* on RMHA (1% wt/vol Eiken agar) after inoculation in the center of 14-cm diameter plates and incubation at 37 °C. (*A*) Twenty-four hours after inoculation of a 10-μL aliquot of spores with conidial germination and outgrowth to form mycelia but no generation of new conidia and limited spread. (*B*) A similar plate 5 d after inoculation with growth of the colony and pigmentation, in part, caused by the formation of new conidia. (*C*) A plate 9 d after inoculation with a larger primary colony and also smaller peripheral colonies (e.g., as indicated by the arrow) that have resulted from airborne spread from the central colony. Under these conditions, it typically took *A. fumigatus* 6–12 d to reach the periphery of the Petri dish. If transported by swarming *P. vortex*, then the leading conidia were able to traverse the same distance in <7 h.

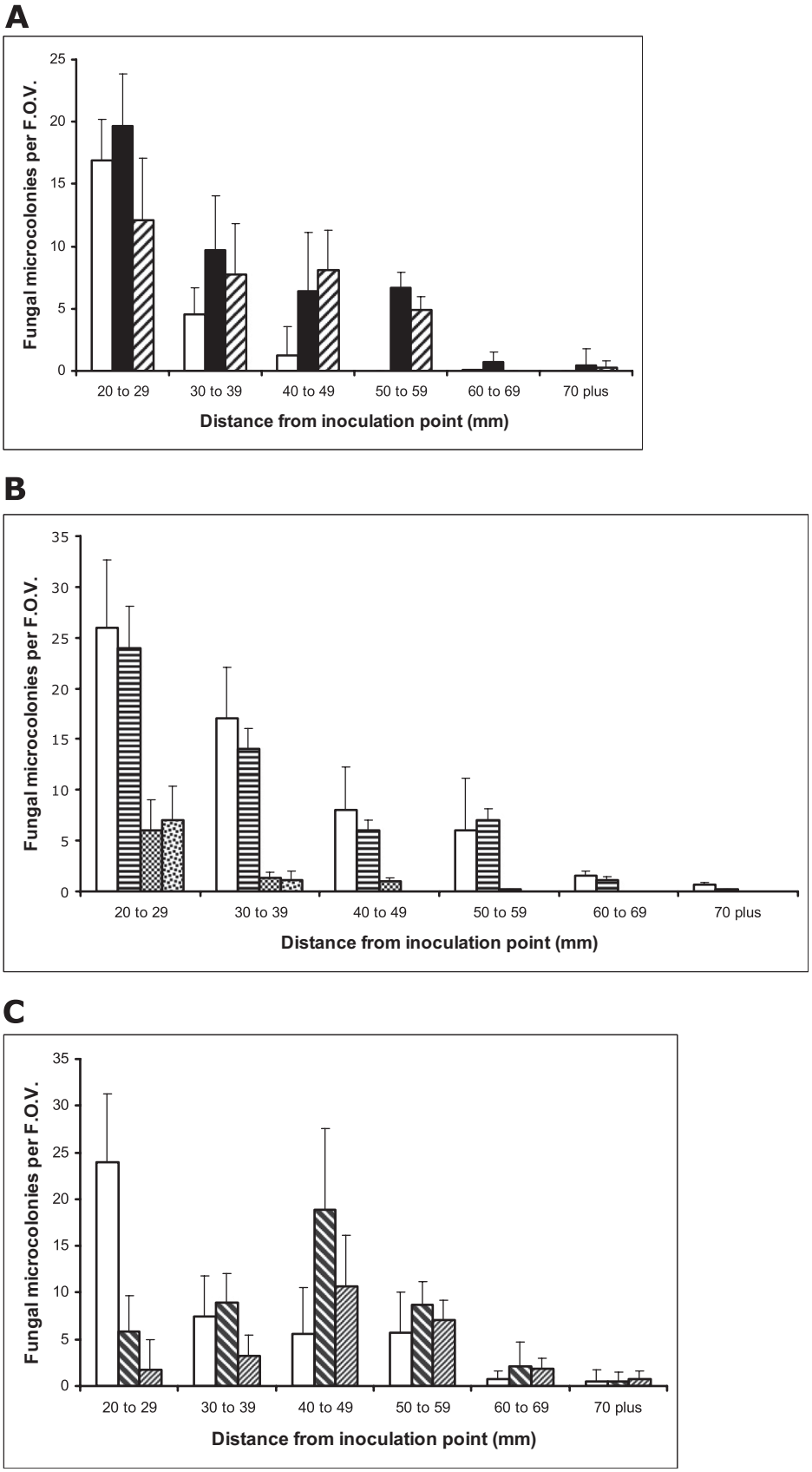

Fig. S4. Quantification of the distribution of *A. fumigatus* microcolonies mediated by swarming *P. vortex* 22 h after coinoculation. Twenty 3 × 4-mm regions within a series of concentric rings surrounding the inoculation point were imaged by low-power microscopy, and the number of fungal microcolonies per field of view (FOV) was counted. Data are means ± SD. Imaging was initiated outside the radius to which *A. fumigatus* could grow from the central inoculation point, either without bacteria or in coculture with *P. vortex* inhibited from swarming using PNPG. (*A*) Effect of different percentage agars (Eiken agar was

Legend continued on following page

used) on distribution with coinoculation of *P. vortex* and ungerminated conidia. White bars, 0.5% (wt/vol) agar. Black bars, 1% (wt/vol) agar. Hatched bars, 1.5% (wt/vol) agar. (*B*) Effect of germination state on transport efficiency on RMHA (1% wt/vol agar). White bars, ungerminated conidia. Horizontally hatched bars, conidia with 2 h pregermination before inoculation. Checkered bars, 5 h pregermination. Stippled bars, 9 h pregermination. (*C*) Effect of antifungal agent voriconazole (VOR) added with the 10-μL inoculation droplet. White bars, no VOR. Boldly hatched bars, 10 μg VOR. Finely hatched bars, 50 μg VOR.

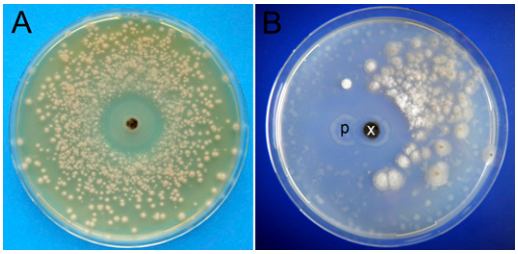

Fig. S5. Rescue of conidia from unfavorable niches. (*A*) *P. vortex* was coinoculated into the central point of a 14-cm diameter RMHA plate with conidia and 30 μg VOR. This amount of VOR was sufficient to inhibit fungal growth within a 27-mm radius from the central point. Despite this fact, *P. vortex* was able to transport conidia, which were then able to germinate and form colonies, outside the zone of inhibition by VOR. In this image (taken 48 h after inoculation), the fungi are visible as white colonies in a background of near-confluent *P. vortex*. The ring-like patterning around the central point is composed of *P. vortex* cells. (*B*) Similar to the image in *A* except that the *P. vortex* was inoculated (P) in a different location to the conidia; the latter had 50 μg VOR (X). The *P. vortex* initiated swarming in all directions in the absence of conidia. Conidia were picked up as bacteria moved over the region X and then deposited in other locations, including those locations outside the zone of effect of the VOR where fungal outgrowth was now possible.

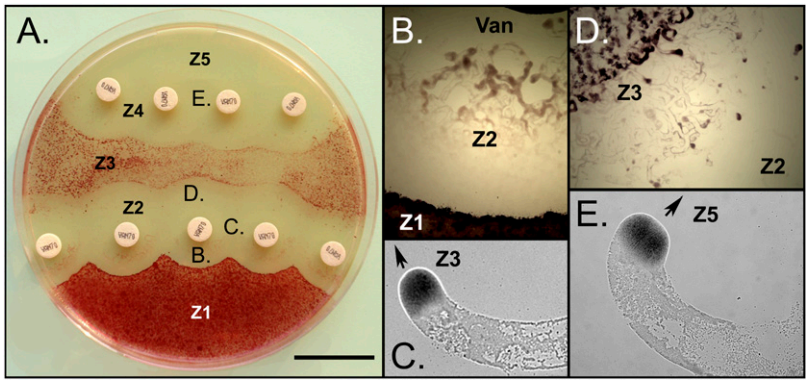

Fig. S6. Experiment showing the ability of pioneering swarming masses of *P. vortex* to cross regions of an agar plate where growth is inhibited by antibiotics to reach more favorable niches. (*A*) RMHA plate (14-cm diameter; 1.5% wt/vol agar) inoculated with *P. vortex* within the center of zone 1 (Z1). Picture was taken after 24 h incubation at 37 °C using a dye (INT) to stain metabolically active bacteria red. Z2 and Z4 are two zones of inhibitory concentrations of VAN created by diffusion of this antibiotic from a series of NeoSensi Tabs. The bacteria rapidly swarm and occupy Z1, but most were limited by VAN from growing and swarming into Z2. However, a limited number of swarming colonies appeared not to be inhibited by VAN and could swarm across Z2 to colonize Z3. The bacteria swarming from Z3 to Z4 were not resistant. Most of those swarming from Z3 into Z4 are affected by VAN in Z4. This finding suggests that stable VAN-resistant mutants were not the explanation for the ability of *P. vortex* to cross Z2. As with Z2, limited numbers could cross Z4 to Z5. By 36 h, Z1, Z3, and Z5 were heavily colonized by *P. vortex*, whereas only small numbers of bacteria could be found in Z2 and Z4. (*B*) Detail from Z1 to Z2 taken with a dissection microscope, with illumination from below showing trails of *P. vortex* close to a VAN NeoSensi Tab. (*C*) Detail from within Z2 taken with an Olympus BX41 microscope showing the trail left by a *P. vortex* mass swarming to Z3 (direction shown by the arrow). (*D*) Same as *B* but showing swarming from Z2 to Z3. (*E*) Same as *C* but showing the swarming mass moving from Z4 to Z5. (Scale bar: *A*, 3 cm; *B* and *D*, 1 cm; *C*, 300 μm; *E*, 220 μm.)

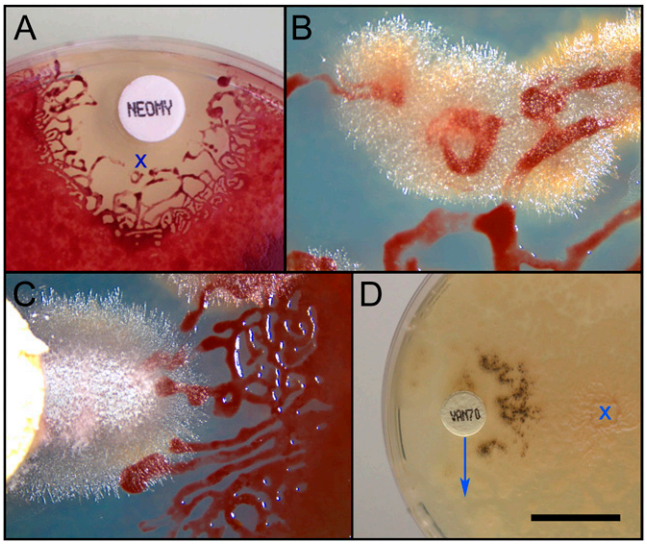

Fig. S7. Transport of viable *A. fumigatus* by *P. vortex* into regions where bacterial growth was limited by an antibiotic. (*A*) Swarming by pioneering masses of *P. vortex* (red) entering the zone of growth inhibition of NEO 12 h after inoculation of both *P. vortex* and *A. fumigatus* conidia at the center of the RMHA plate. (*B*) Detail from *A* (location marked by the X) imaged after 20 h. Outgrowth of *A. fumigatus* from conidia carried by *P. vortex* into the region of neomycin action was now visible. (*C*) Similar to *B* but showing outgrowth of transported *A. fumigatus* from *P. vortex* (the latter is now partially obscured by fungal mycelia) adjacent to a VAN NeoSensitab. (*D*) RMHA inoculated with both organisms imaged after 52 h. The zone of inhibition of VAN was visible after 18 h (radius shown by the arrow) but by 52 h, was largely obscured by fungal growth. By this time, fungal colonies were visible across the plate, but production of dark green conidia by *A. fumigatus* was only observed within the original zone of growth inhibition of VAN. This finding remained the case after 100 h.

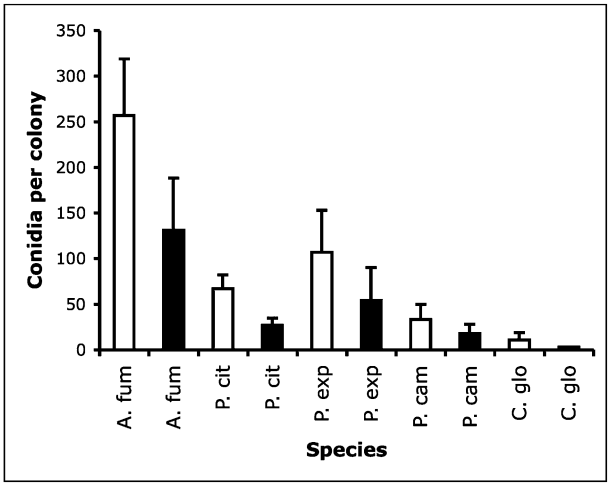

Fig. S8. Transport of conidia from different filamentous fungi assessed by microcopy of *P. vortex* colonies (average of five colonies) on RMHA at 37 °C. Black bars, analysis of colonies 1–2 cm from inoculation point after 90 min; white bars, colonies assessed 2–4 cm from inoculation point after 150 min. A. fum, *A. fumigatus*; C. glo, *C.* gloeosporioides f. sp. *aeschynomene* 3.1.3; P. cam, *P. camemberti* LCP 66.584; P. cit, *P. citrinum*; P. exp, *P. expansum*.

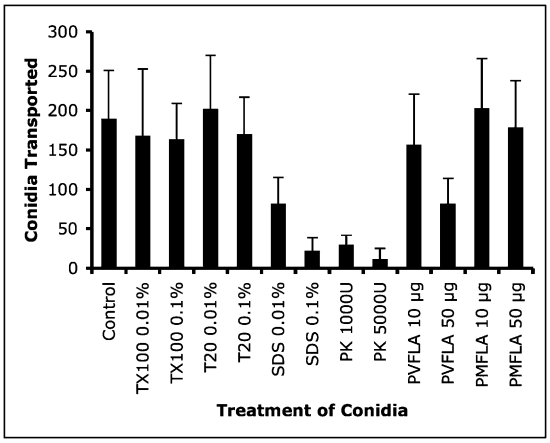

Fig. S9. Effect of pretreatments of *A. fumigatus* conidia on transport by *P. vortex*. Conidia were incubated with a detergent, protease, or purified flagella as described in *SI Materials and Methods*. The conidia, after washing, were then used in transport assays, scoring the number of conidia per swarming microcolony 3 h after coinoculation with *P. vortex*. Swarming bacterial colonies (1–2 cm from the inoculation point; average of three replicate plates ± SD) were harvested by toothpick and applied to microscope slides, and the number of cargo conidia was counted. PK, proteinase K; PMFLA, flagella from swarming *P. mirabilis*; PVFLA, flagella purified from swarming *P. vortex*; T20, Tween-20; TX100, Triton ×100. Detergent concentrations are expressed as percentage (wt/vol). Protease units and amounts of flagella are the amount present in the 1-mL volume with 10^8 conidia. None of the conditions tested inhibited the swarming of the *P. vortex* coinoculated with the conidia.

Table S1. Velocity estimates of conidia (mm h^{-1}) derived from movies compared with virtual objects (Fig. 3)

	Pair 1	Pair 2	Pair 3	Pair 4	Pair 5
Conidia	7.98 ± 0.61	8.40 ± 0.46	8.90 ± 0.65	8.68 ± 1.84	11.26 ± 1.07
Virtual	9.70 ± 1.39	9.69 ± 0.77	8.78 ± 1.02	10.44 ± 0.70	11.32 ± 0.62

The velocity calculations are the mean ± SD of 90 pairwise comparisons between successive frames.

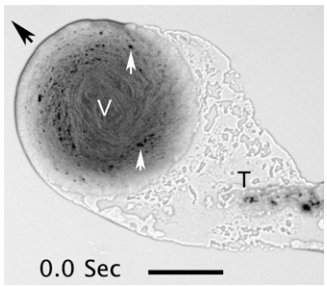

Movie S1. Time-lapse movie showing mass conidial transport by *P. vortex* swarming as a rotating colony 2 h after inoculation. T, trail of cells and lubricant material; V, rotating colony (rotating clockwise one time every 12 min). Conidial masses (e.g., dark objects indicated by the white arrows containing 10–100 conidia) are rotating at ~3 μm s^{-1} (11 mm h^{-1}). Black arrow shows overall direction of progress of the colony (over a longer time period than covered by this movie). (Scale bar: 500 μm.)

Movie S1

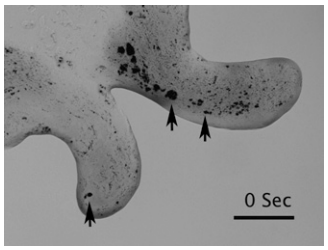

Movie S2. Swarming mass of *P. vortex* transporting hundreds of ungerminated conidia (dark masses; e.g., indicated by arrows) imaged 4 h after inoculation and 31 mm away from the coinoculation point. (Scale bar: 300 μm.)

Movie S2

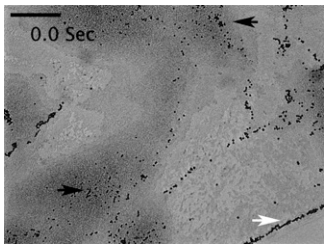

Movie S3. Swarming mass of *P. vortex* transporting hundreds of ungerminated conidia (individual moving conidia are visible; e.g., indicated by black arrows). Not all conidia are in motion (e.g., row of deposited conidia indicated by the white arrow). (Scale bar: 100 μm.)

Movie S3